

## Laser-induced glass-crystallization phenomena of GeSe<sub>2</sub> investigated by light scattering

E. Haro, Z. S. Xu, J.-F. Morhange, and M. Balkanski

*Laboratoire de Physique des Solides, Université Pierre et Marie Curie, 4 place Jussieu, F-75230 Paris (Cédex) 05, France*

G. P. Espinosa and J. C. Phillips

*AT&T Bell Laboratories, Murray Hill, New Jersey 07974*

(Received 19 June 1984)

Recrystallization of glassy GeSe<sub>2</sub> under laser irradiation has been studied with use of Raman spectroscopy. A threshold irradiation power level below which no changes in the local molecular structure of the system can be detected has been defined. For an irradiation power above the threshold, three stages of transformation have been identified: The first stage is characterized by the nucleation of clusters or submicrocrystallites which remain embedded in a continuum glass matrix. The second stage is characterized by the coexistence of clusters of various sizes. Up to this stage, the system is fully reversible. The last stage is reached when the crystallites coalesce to form a polycrystalline material.

### I. INTRODUCTION

The molecular structure of chalcogenide alloy glasses As<sub>x</sub>Se<sub>1-x</sub> and Ge<sub>y</sub>Se<sub>1-y</sub> has been extensively studied by Raman<sup>1-10</sup> and Mössbauer spectroscopy.<sup>11-15</sup> Diffraction studies<sup>16,17</sup> have shown that near the crystalline compositions the short-range order of these glasses is similar to that of the crystalline compounds. Recent Raman<sup>9,10</sup> and Mössbauer<sup>11-15</sup> data have extended this result to include a large number of atoms (intermediate-range order). These studies have identified atomic sites and bonds both in the interior and on the surface of large clusters (diameters of order 50–100 Å). The interiors of these clusters have crystalline topologies, as evidenced by close correspondence of their Raman band and Mössbauer site signatures with the crystalline values.<sup>18</sup>

One of the central questions in glass science is the microscopic or molecular origin of the kinetic barrier which frustrates crystallization in materials which are good glass formers. Recently Griffiths *et al.* have examined this question for *g*-GeSe<sub>2</sub> and *g*-Ge(S<sub>x</sub>Se<sub>1-x</sub>)<sub>2</sub> alloys by Raman scattering.<sup>10,19</sup> According to their results the crystallization process narrows and shifts the strongest Raman bands in the glass, while other moderately strong Raman bands associated with broken chemical order disappear. The later stages of crystallization show many narrow Raman bands where only very broad bands were present before. Because the crystalline unit cell contains 48 atoms, all the crystalline bands cannot be identified in detail. However, all the observed behavior is consistent with previous assignments of glass modes to normal tetrahedral and broken chemical-order modes as required by composition dependence of Raman and Mössbauer spectra. Moreover, they were able to monitor the laser-induced crystallization process at  $T \sim 100K$  and show that it was at least a two-stage process which could be thermally reversed at temperatures as low as  $T_g/2 \sim 200K$ . An important feature of their experiment was the use of 1.9-eV pump radiation which lies below the band gap

of 2.2 eV. They also used low-power levels and long pulses (3 min) to induce structural transformations.

In the present work, we use laser irradiation to induce structural transformations in the glass and we probe the resulting effects with a light scattering experiment. A preliminary account of our observations has already appeared.<sup>20</sup>

Two laser sources argon and krypton of energies 2.4 and 1.9 eV, well above and well below the band gap, respectively, were used. The penetration depth<sup>21</sup> at the 1.9-eV laser energy used by Griffiths *et al.*<sup>10,19</sup> is close to 30 μm, whereas at 2.4 eV, the penetration depth is close to 0.5 μm. These large differences in penetration depth at ambient temperature were expected to modify substantially the kinetic phenomena, especially in the delicate reversible glass-microcrystalline region.<sup>22-24</sup>

The progressive transformations evidenced by the Raman spectra revealed the evolution of the system through the following steps:

(i) As the energy input in the system grows, the number and the size of clusters randomly nucleated increases. The observed line narrowing of the internal mode  $A_1$  of the clusters (220 cm<sup>-1</sup>) indicates an enlargement of the clusters and constitutes a precursor effect.

(ii) When the size of the individual cluster becomes sufficiently large, decreasing thereby the average spacing between different clusters, the clusters coalesce randomly in a percolation transition into small crystallites. This is demonstrated by an increase in the intensity of the crystalline normal mode vibration line (210 cm<sup>-1</sup>). At this stage, the system remains reversible and without further input of radiation energy, crystallization is prevented by relaxation of the individual clusters toward the glass state. This is a clear demonstration of a dynamical reversal effect.

(iii) With further increase of the input irradiation power the number of coalescing clusters rapidly increases until the system is definitely clamped into the crystalline state which then remains stable.

Apart from the clear definition of the successive phases in the organization of the glass, our investigation shows that each significant step is a threshold phenomenon. The system undergoes a slow evolution before a threshold energy density is reached above which the ordering phenomenon rises rapidly with input power.

## II. STRUCTURAL TRANSFORMATIONS IN $\text{GeSe}_2$ GLASS AND THEIR OBSERVATION BY LIGHT SCATTERING

Light scattering is one of the most powerful tools for studying the structure of disordered solids.<sup>25,26</sup> This method is of particular interest in the investigation of the transformations between disordered and crystalline phases which can be followed by the correlation between broad bands characteristic of the disordered state and narrow peak pertinent to the crystal structure. Light scattering reveals the vibrational and rotational modes of the system. The dynamical behavior is closely related to the immediate environment of the atomic sites. It is therefore a direct probe of the molecular structure and the mutual arrangements of the individual molecules.

Recently, great attention has been focused on materials  $\text{GeS}_2$  and  $\text{GeSe}_2$  whose Raman spectra have been studied in great detail.<sup>1-8</sup> In a major interpretive advance it was shown<sup>9</sup> that all the available data do indeed point to the presence of large partially polymerized clusters in  $g\text{-GeS}_2$  and  $g\text{-GeSe}_2$  and that many of these large clusters are fragments of the high-temperature layer structures which are terminated on their lateral edges by chalcogen dimers. Many of the structural details of this model have been clarified and extended by Mössbauer studies.<sup>11,12</sup>

Measured Raman spectra of  $c\text{-GeSe}_2$  have been used earlier<sup>9</sup> to analyze the spectra of  $g\text{-GeSe}_2$ . This work has confirmed previously established correspondences<sup>10</sup> between the tetrahedral normal modes (symmetry labels  $A_1$ ,  $E$ ,  $F_2$ , and  $F_2$ ) and four peaks in the Raman spectrum of  $g\text{-GeSe}_2$ . It has also been established that a fifth line at  $214\text{ cm}^{-1}$  has a similar behavior to that of the tetrahedral  $A_1$  symmetric breathing mode at  $200\text{ cm}^{-1}$  which involves only chalcogen motion. Bridenbaugh *et al.*<sup>9</sup> have designated the fifth line as "the companion  $A_1$  Raman line." The model which explains the origin of the companion  $A_1$  line is based on the assumption that the structural unit in  $g\text{-Ge}(\text{S}_1\text{Se})_2$  is a large cluster which is a fragment of the layer crystal structure still polymerized along the  $a$  axis but is terminated along the  $b$  axis by Se dimers, as shown in Fig. 1.

Aronovitz *et al.*<sup>27</sup> and Murase *et al.*<sup>8</sup> have calculated the vibrational modes of these large clusters and attempted to relate them to the Raman spectra of the crystal and the glass. There are 24 atoms in the unit cell and nearly 70 Raman active modes could be expected. The identification of all the normal modes is a difficult and in many cases also unrewarding task. It is far more interesting to follow some dominant modes which could bring useful information on the glass-crystalline transformation.

In this work, we shall investigate essentially the effect of laser power beam on the structural transformations of  $\text{GeSe}_2$  glass by following the bandwidth and intensity

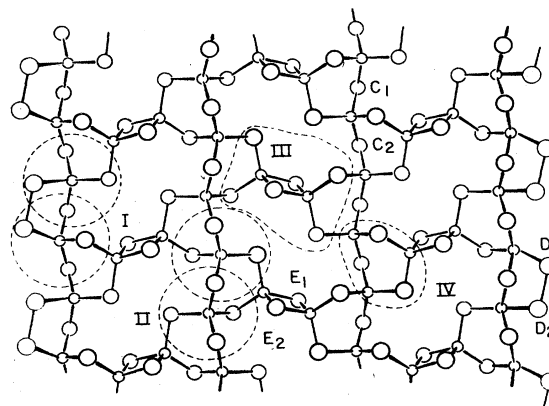


FIG. 1. Structure of a glass cluster in  $\text{Ge}(\text{S},\text{Se})_2$ . The companion  $A_1$  line, denoted by  $A_{1C}$ , is associated with the vibrations of tetrahedra linked by chalcogen dimers, indicated by  $I$  here (figure from Ref. 27).

variations of the peaks at  $210$  and  $200\text{ cm}^{-1}$  in connection with the interaction between the clusters and their coalescence.

## III. EXPERIMENTAL PROCEDURE

Experiments have been performed on melt-quenched  $\text{GeSe}_2$  samples supplied by AT&T Bell Laboratories. The preparation procedure is described elsewhere.<sup>19</sup> The samples have been subjected to measurements at room temperature in air.

Raman spectra were recorded using a double monochromator (Coderg PHO) with a classical photon-counting detection system. Two different laser wavelengths were used in these experiments: The first line was the  $5145\text{-\AA}$  ( $20410\text{-eV}$ ) line from a Coherent RAD CR2 argon laser. The other was the  $6317\text{-\AA}$  ( $1.916\text{-eV}$ ) line from a Spectra Physics model 164 krypton laser. In both cases, the spectra were recorded in a reflection geometry. Unless otherwise stated, the pump  $P_I$  and probe  $P_R$  laser wavelengths were the same in a given experiment. The probe intensity  $P_R$  was low enough not to alter the spectra during recording while the pump intensity  $P_I$  was increased to induce structural changes.

## IV. EXPERIMENTAL RESULTS AND DISCUSSION

### A. Precursor effect

The series of light scattering spectra shown in Fig. 2 represent different stages of irradiation of  $g\text{-GeSe}_2$ . The samples are irradiated with a laser beam of energy  $2.4\text{ eV}$  well above the  $2.2\text{-eV}$  absorption edge of the material<sup>19</sup> at room temperature. The laser spot on the sample has a diameter of  $100\text{ }\mu\text{m}$ . The incident laser energy density is monitored by means of an attenuator.

The reference Raman spectrum 2(a) is recorded with a probe beam of  $P_R = 9\text{ mW}$  which does not induce any structural changes in the glass. This point is confirmed

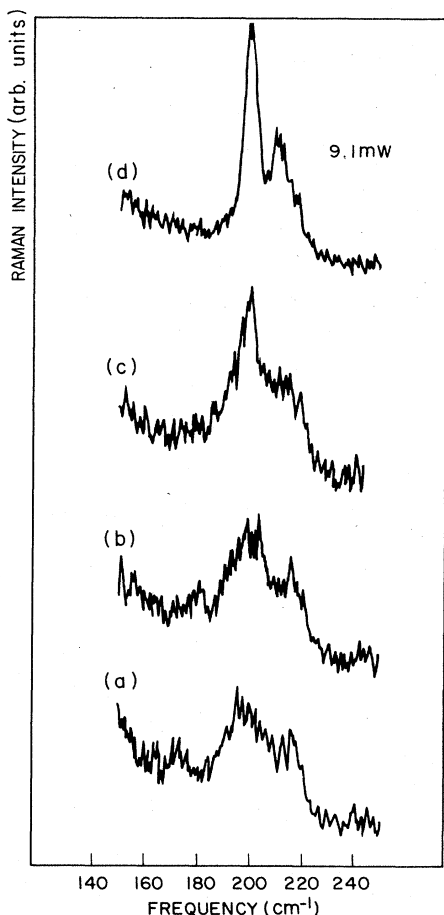


FIG. 2. Transformation of the  $A_1$  region of the Raman spectrum (a) with probe power 9 mW only, (b) with pump power 18.2 mW, (c) 22.8 mW, and (d) after longer irradiation at 22.8 mW. Power of the probe laser recording beam fixed at 9 mW.

by repeating the recording at sufficiently larger intervals without observing any significant changes in the spectrum. Three bands are observed, centered at 172, 200, and 217  $\text{cm}^{-1}$ . We are considering here the spectral region between 150 and 250  $\text{cm}^{-1}$ . The most prominent band here is centered at 200  $\text{cm}^{-1}$ , designated<sup>9,10</sup> as the  $A_1$  cluster Ge—Se vibrational mode in GeSe<sub>2</sub>. A variety of studies, both by Raman<sup>9</sup> and Mössbauer<sup>14</sup> spectroscopy, have associated the 172 and  $A_{1C}=215$   $\text{cm}^{-1}$  bands with Ge—Ge and Se—Se bonds, respectively, although the normal modes of vibration are not necessarily well localized on these atom pairs.<sup>27</sup>

Only in small clusters will the surface bands such as  $A_{1C}$  have intensity comparable to that of the inner-cluster modes  $A_1$ . As the cluster size increases, the inner mode density will dominate because the number of the sites inside the cluster with corner-sharing tetrahedra will increase more rapidly than that of outer chains (surface/volume effect). This effect is shown in the spectrum

2d where the intensity of the internal 200- $\text{cm}^{-1}$   $A_1$  mode dominates up to the point where the 172- $\text{cm}^{-1}$  Ge—Ge mode is not resolved anymore.

The spectrum shown in 2(b) is recorded after an irradiation with a laser beam of power  $P_I=18.2$  mW. The spectrum 2(c) is recorded after an irradiation with incident power  $P_I=22.8$  mW. We observe a narrowing and increase in intensity of the inner  $A_1$  mode of the cluster which is a demonstration of the tendency for the enlarged clusters to form microcrystallites enlarging the dimensions of the clusters, thus favoring the ratio of bulk to surface modes. The band narrowing is an indication that the network of corner-sharing tetrahedra is beginning to form a crystal lattice. Further irradiation of the sample enhances even more this tendency, as can be seen in the spectrum 2(d) recorded after a second irradiation with  $P_I=22.8$  mW. This irradiation of a longer duration has led to a more persistent effect. The spectrum recorded with a probe beam of  $P_{R_1}=9.1$  mW shows a dramatic narrowing of the peak at 200  $\text{cm}^{-1}$  having a half linewidth  $\Gamma_{200}=4$   $\text{cm}^{-1}$  which is typical for crystalline material. In addition, the normal-mode Raman active peak of crystalline<sup>9</sup>  $c$ -GeSe<sub>2</sub> at 210  $\text{cm}^{-1}$  appears at this stage.

Some quantitative changes can also arise from effects of the radiation field. Because the energy of the incident beam lies above the absorption edge, it is strongly absorbed near the surface of the material and does not penetrate more than 100 Å. Electronic transitions occur and bonds may break. Nevertheless, we consider that electronic effects are of secondary importance for the spectral changes under examination which essentially involve structural transitions on the molecular level (clusters of atoms). The transformations occurring in this case are rather a consequence of the softening of some of the inter-cluster interactions which give more rotational freedom to the system. The thermal energy transferred to the system in the form of cluster rotational excitations leads to the possibility of further network reconstruction at the surface of a small cluster, thus enlarging the existing clusters and also giving the opportunity for new clusters to nucleate.

A very important feature of this experiment is the discovery of a *precursor effect* in the glass-to-crystalline transition. It is expressed by the sharp narrowing and the intensity increase of the 200- $\text{cm}^{-1}$  peak due to the inner-glass-cluster mode which just precedes the transformation of clusters into microcrystallites. This is just on the stage where the first sign of crystallization appears with the start to rise in the intensity of the crystal peak at 210  $\text{cm}^{-1}$ . We are now in a highly nonequilibrium state. The system left on its own will slowly self-anneal and return to the glass state, but on further irradiation, it will tend towards the crystalline state. The precursor effect indicates crystallization if the conditions which brought the precursor are maintained.

#### B. Intensity increase effect

When the radiation power is increased, two types of effects are observed. One is the intensity increase and even-

tual narrowing of certain bands and the second is the disappearance of certain Raman bands and the appearance of new Raman lines. Both of these effects signal structural transformation of the glass under laser irradiation. Their evolution is gradual and this makes it possible for us to study intermediate nonequilibrium states. An almost complete picture of these transformations is given in Fig. 3. With relatively low-radiation power  $P_I=3.6$  mW, we observe in the spectrum 3(a) the main features already described for the glass material. At this laser intensity, no transformation occurs in the glass. When the radiation power is increased and a beam of  $P_I=7.2$  mW is used, the recorded spectrum 3(b) shows an increase in the light scattering strength without modification in the shape of the spectrum. The density of modes contributing to the

light scattering is increased but their nature remains the same. This process is called photodarkening; it is probably associated with the creation of transient electronic traps which stimulate cluster rotation.<sup>28</sup> At this stage no structural changes are discernible in the Raman spectra.

The spectrum 3(c) is recorded with an incident laser power of  $P_I=21.6$  mW. A significant narrowing of the band at  $200\text{ cm}^{-1}$  is clearly observed here and one can almost discern a shoulder at  $210\text{ cm}^{-1}$ .

Further increase in the power of the incident beam leads suddenly to substantial changes in the spectrum: under irradiation with a beam of  $P_I=24$  mW, the recorded spectrum 3(d) shows clearly two peaks at  $200$  and  $210\text{ cm}^{-1}$ . While the Raman peak at  $200\text{ cm}^{-1}$  due to the inner-cluster mode  $A_1$  still persists, one sees clearly a new peak at  $210\text{ cm}^{-1}$ . This simultaneous observation demonstrates the coexistence of two phases; on one side, large glass clusters attested by the persistence of the peak at  $200\text{ cm}^{-1}$  and on the other side, microcrystallites large enough to show the peak corresponding to the normal mode in the crystal lattice of  $c\text{-GeSe}_2$ , obeying the  $k=0$  selection rule.

As shown in spectrum 3(e), irradiation under a power beam  $P_I=26.4$  mW produces steady growth of the crystalline phase but the peak at  $200\text{ cm}^{-1}$  still persists. The picture that one may get from this spectral data is that increasing the incident laser power leads to the formation of crystallites which coexist with the clusters in the glass phase. The clusters transform gradually. Some of them may grow by addition of newly oriented molecules to their surfaces, others may fuse together to form larger clusters of microcrystallites which are still embedded in the glass. The distance scales for these different formations may be estimated as follows. Suppose that the clusters are about  $50\text{ \AA}$  in diameter,<sup>2</sup> then the critical Gibbs diameter for nucleation of microcrystallites would be about  $150\text{ \AA}$  for  $\text{GeSe}_2$  (Ref. 29) and formation of crystallites will occur when the diameter becomes larger than  $200\text{ \AA}$ . Above this size, polycrystalline regions separate and macroscopically distinct from the glass regions may form.

In the beginning of this sequence, only a few microcrystallites have formed, let us say a fraction of  $0.1$  ( $f_c \sim 0.1$ ) which would be too few to give enough intensity to the band at  $210\text{ cm}^{-1}$ . Now there is an important difference between the crystal and the glass as regards<sup>30</sup> density  $\rho$ . The density of the crystal is  $\rho_c = 1.1\rho_g$ . When  $f_c$  is of the order  $0.1$ , in effect about less than  $1\%$  of the surrounding glass becomes "free volume." Many phase transitions involve density changes of a few percent. Thus we expect that when the free volume increases above  $1\%$  the  $50\text{-\AA}$  clusters may be much freer to rotate than they were before.<sup>31,32</sup> As a result, a number of the smaller clusters will fuse together to form larger clusters, with an average size which increases rapidly.

The evolution of the light scattering spectra suggests that we have to consider three states with regard to the structure of the material. The first is the equilibrium glass state where the contribution to the light scattering is essentially from localized molecular types of vibrations. The third is the crystal state, where light scattering occurs through normal lattice vibrational modes characteristic of the infinite crystal with translational invariance. The

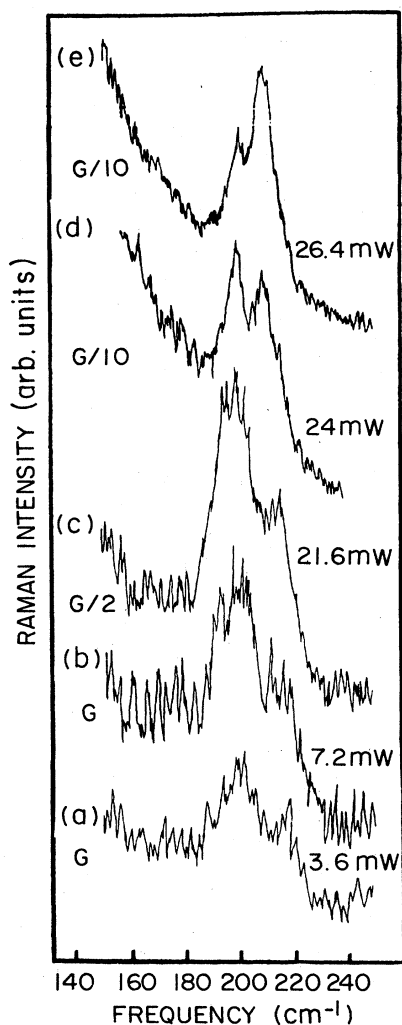


FIG. 3. Transformation of the  $A_1$  spectrum with more closely spaced power levels in the critical region just above  $P_I=20$  mW. Again the recording power is fixed at  $9\text{ mW}$ . Here and in later figures the gain level of the detector is denoted by  $G$ .

second state is an intermediate state where clusters ( $\lesssim 100$  Å in diameter) embedded in the glass matrix coexist with metastable three-dimensional microcrystallites with a diameter of the order of 150 Å as well as crystallites large enough to be stable. The continuous transformation between the first and second stage is characterized by the size of the clusters. In the glass, the clusters are formed by a small number of molecular units equivalent to a few elementary unit cells, for example. If these clusters were undeformed, then we would expect the usual  $k=0$  selection rules for Raman scattering to apply, except that a range of  $k$  near  $k=0$  would be optically active, with  $|k| \lesssim R^{-1}$ ,  $R$  being the cluster diameter. This is the intrinsic line broadening due in effect to the uncertainty principle. Because the glass structure is microscopically ductile (the number of atomic force field constraints is nearly equal to the number of atomic degrees of freedom),<sup>26</sup> each cluster is expected to be substantially deformed (although its network topology is still crystalline) and this gives rise to further extrinsic broadening. As the cluster size grows, both sources of band broadening are reduced. The corresponding light scattering line will be substantially narrowed. Increasing further the dimensions of the structural unit, the linewidth will continue to decrease until we reach the linewidth of a Raman active normal mode obeying  $k=0$  selection rule. In this case, the light scattering intensity will also be considerably increased. This is a mechanism for band narrowing and intensity increase for the peak at  $200\text{ cm}^{-1}$ . The peak at  $210\text{ cm}^{-1}$  appears only for structures with  $d > 150$  Å corresponding to the crystal normal modes of vibration.

### C. Threshold for microcrystallite and crystallite formation

Another demonstration of the continuous evolution of the system as the incident laser energy density increases is given in Fig. 4. With an incident energy density at a sufficiently low level  $P_I = 13.20$  mW, when no significant changes in the system have occurred, the spectrum is that of *g*-GeSe<sub>2</sub> shown in Fig. 4(a). When the incident energy density is increased, the evolution of the spectrum is shown consecutively in Figs. 4(b), 4(c), and 4(d) for incident beams  $P_I^b = 35$  mW,  $P_I^c = 39.6$  mW, and  $P_I^d = 48$  mW, respectively. The intensity of the crystalline peak at  $210\text{ cm}^{-1}$  does not reach its final value immediately after the power of the laser beam is incident on the sample:  $t_1$  is the instant at which a laser beam of a given power is incident and  $t_2$  is the "stabilization time," i.e., the time after which the Raman spectrum has reached a nearly constant value and remains stable. Figure 5 shows the variation of the Raman intensity of the peak at  $200\text{ cm}^{-1}$  characteristic of the internal tetrahedral  $A_1$  vibrational mode of the cluster. For relatively low power of the incident laser beam, the Raman intensity changes very slowly with increasing power, whereas the intensity rises abruptly beyond a certain power level. Above a threshold power, the density and the size increase of the clusters develops very rapidly. Figure 5 shows the same threshold behavior for the crystallite formation. In this figure, a dramatic increase of the intensity of the crystalline peak

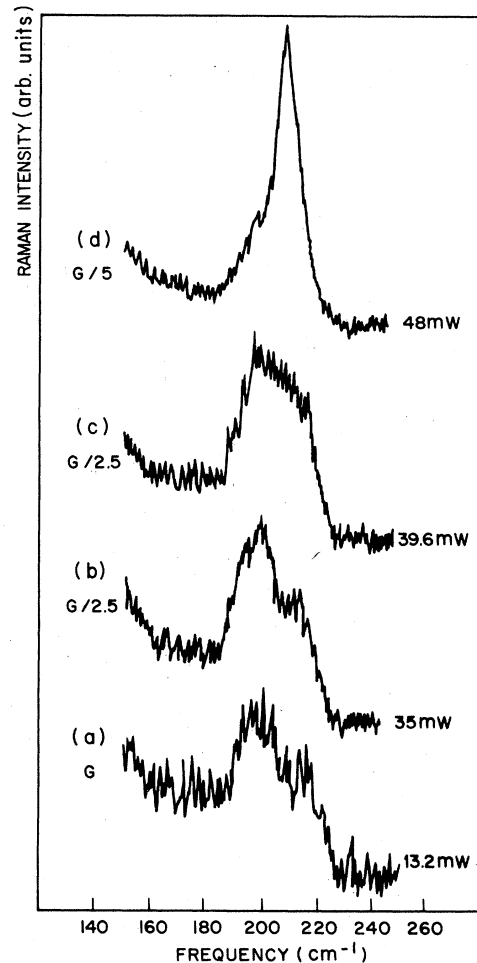


FIG. 4. Similar to Fig. 3 but with shorter exposure times, so that the critical power level is higher.

at  $210\text{ cm}^{-1}$  is shown above a certain incident laser power. Below the threshold power, the crystalline peak is scarcely discernible, but as soon as a power of 25 mW is reached, the intensity of the  $210\text{-cm}^{-1}$  peak rises sharply. From the curves shown in Fig. 5, it is possible to deduce the threshold power for cluster microcrystallite formation  $E_{th}^m = 21$  mW and the threshold power for crystallite formation  $E_{th}^c = 25$  mW.

Below threshold, no changes in the structure of the Raman spectrum are observed. The overall intensity of the spectrum increases slightly with the increase of incident power but the shape of the bands remains unchanged. As soon as threshold power is reached, band narrowing occurs and the line intensity increases very rapidly with incident power. In the case of the crystalline peak at  $210\text{ cm}^{-1}$ , the effect is even more dramatic. Below threshold ( $E_{th}^c = 25$  mW), the peak at  $210\text{ cm}^{-1}$  is not observed, but as soon as threshold is reached a peak at  $210\text{ cm}^{-1}$  appears in the spectrum and its intensity rises far more rapidly than that of the peak at  $200\text{ cm}^{-1}$  as power increases. Ultimately, the peak at  $210\text{ cm}^{-1}$  dominates with such a great intensity that no peak at  $200\text{ cm}^{-1}$  is perceptible.

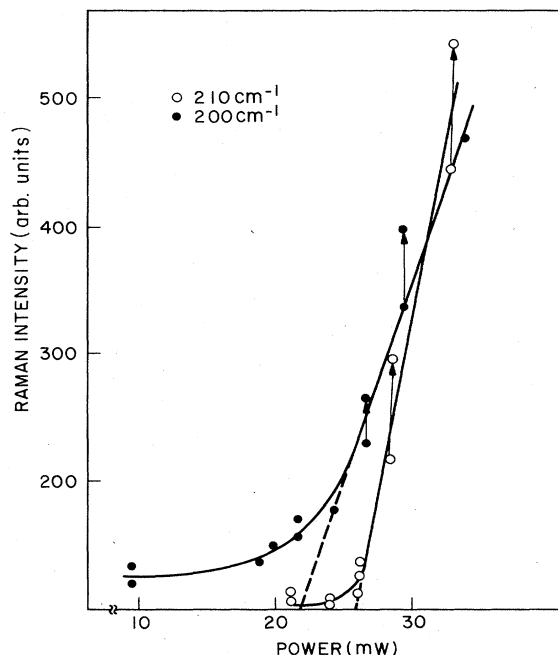


FIG. 5. The glass band at  $200\text{ cm}^{-1}$  narrows and its peak height grows before the crystalline band at  $210\text{ cm}^{-1}$  appears. The thresholds for the glass and crystalline bands are nearly 21 and 26 mW, respectively, according to the dashed lines.

#### D. Nonequilibrium kinetics

The most significant effect in this investigation is the observation of the coexistence or the continuous transformation of the three phases: glass, microcrystallites, and crystal. This observation is illustrated by the spectra given in Fig. 6. The spectrum shown on the bottom of Fig. 6(a) is the reference spectrum of the glass stage. This spectrum is taken under irradiation at a power of  $P_I = 9.9\text{ mW}$ . This spectrum recorded for irradiation below the threshold power remains unchanged if the radiation is maintained at this level even for long times. The spectrum recorded as soon as the incident intensity is increased to a power of  $25.4\text{ mW}$  is shown in Fig. 6(b). No drastic changes are observed in comparison with the spectrum 4(a) except for a general increase in intensity. Ten minutes of irradiation with the same intensity ( $P_I = 25.40\text{ mW}$ ) induces only a slight narrowing of the band due to the inner-cluster mode at  $200\text{ cm}^{-1}$  but the surface-cluster mode near  $215\text{ cm}^{-1}$  still persists as can be seen in the spectrum 6(c). At this stage we can say that for relatively low-energy density very near the threshold energy and sufficient time of irradiation a certain number of clusters are formed and some of them are sufficiently enlarged that some narrowing of the band at  $200\text{ cm}^{-1}$  is perceptible. After 60 minutes of irradiation with the same power, the picture changes completely [see spectrum 6(d)]. The band at  $215\text{ cm}^{-1}$  disappears and a new peak arises at  $210\text{ cm}^{-1}$  which is the frequency of the normal mode of vi-

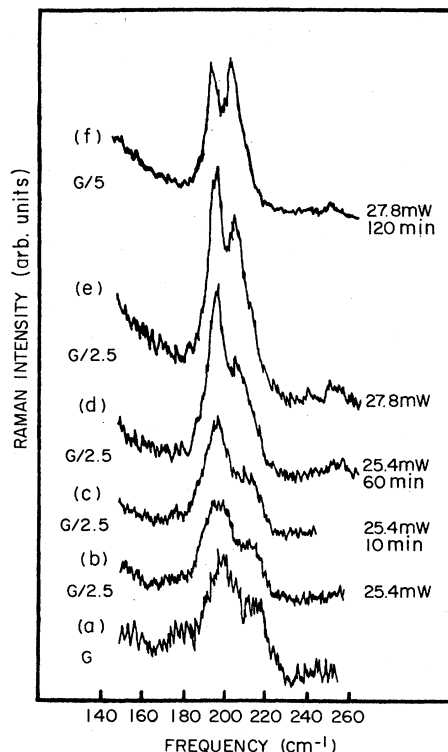


FIG. 6. The effects of varying exposure times near threshold.

bration of  $c\text{-GeSe}_2$  and the peak at  $200\text{ cm}^{-1}$  is now significantly narrowed. This spectrum demonstrates that for a long enough time with an irradiation just above the threshold energy, large crystallites are formed under irradiation, although enlarged clusters still persist embedded in the glass. The recording 6(d) represents a sort of pre-crystallization state. The irradiation power is just at the threshold energy. The band at  $200\text{ cm}^{-1}$  attesting the existence of incipient microcrystallites which is now a narrow peak remains practically constant with time. The crystalline peak at  $210\text{ cm}^{-1}$  has just appeared demonstrating the existence of crystallites which remain in equilibrium with the microcrystallite density as long as the radiation power remains just at the threshold energy. Further increase of the incident radiation energy density even by a very small amount induces immediately a drastic change in the picture. The spectrum 6(e) is recorded with a radiation power of  $P_I = 27.8\text{ mW}$ . The two peaks reflecting the microcrystalline state ( $200\text{ cm}^{-1}$ ) and the crystalline state ( $210\text{ cm}^{-1}$ ) are now in competition. Continuous irradiation at the same power ( $P_I = 27.8\text{ mW}$ ) for 120 minutes gives rise to the spectrum shown in Fig. 6(f) which reflects again a "metastable" situation. Practically equal amounts of microcrystallites having small dimensions  $d < 150\text{ \AA}$  and crystallites which are larger-ordered region with  $d > 150\text{ \AA}$  remain in metastable equilibrium as long as the radiation power is maintained at the same level. An increase of the radiation power will lead to a sudden rise of the peak at  $210\text{ cm}^{-1}$  to an extent such that

the 200 cm<sup>-1</sup> band will be hardly perceptible. The system will transform into the crystalline state which, if the irradiation power is sufficient, will be a thermally irreversible state. On the contrary, if the radiation is withdrawn the system tends to return to its initial state. The microcrystallites are dissolved into the glass state. The kinetics observed here are still far removed from equilibrium in the sense that the evolution of the system towards the ordered state requires a continuous energy input at an increasing rate. Even when the transformation is triggered, if the energy supply is stopped, the system will revert to the glassy state. The intermediate state can be steadily maintained against thermal reversion only under constant supply of external energy. The kinetic evolution is not describable in terms of near-equilibrium relaxation processes, and we observe metastable states under well-defined external conditions. If these conditions are withdrawn, the system evolves toward its disordered state.

#### E. Crystallization time dependence

The irreversible crystalline state is obtained for irradiation power above the threshold energy level applied for a sufficiently long time. Definite recrystallization can also be obtained with very short pulses of higher-power levels.

The two extrema equilibrium states as revealed in a Raman spectrum are shown in Fig. 7. Spectrum 7(a) is that of the glass recorded under low radiation power  $P_I < 10$

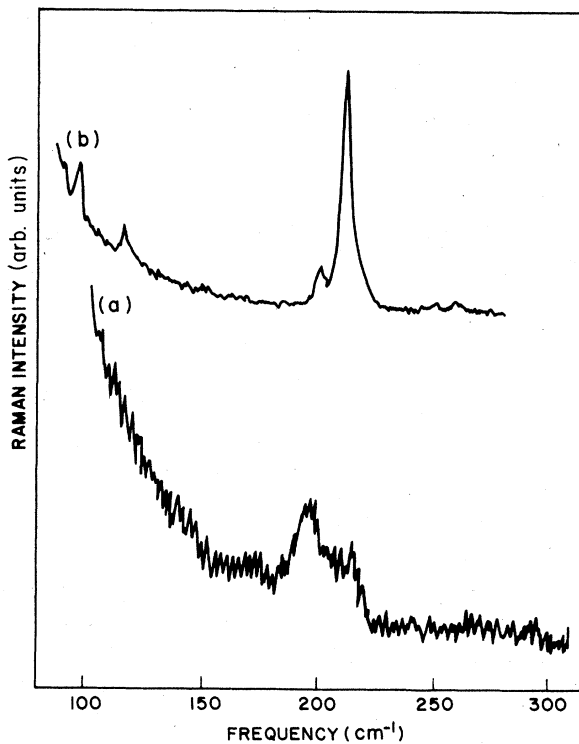


FIG. 7. With high power levels the glass spectrum (a) is transformed to the crystalline spectrum (b) in 1 min.

mW. The spectrum 7(b) is recorded after one minute of irradiation at a high-power level. It represents the spectrum of the crystal GeSe<sub>2</sub>.

The time dependence of the transformation between these two extrema is observed in the following way. The sample is irradiated with a laser beam of energy 2.40 eV. The spot has a diameter of  $\sim 100 \mu\text{m}$ . The power beam is  $P_I = 100 \text{ mW}$  and the spectra are recorded with a probe laser beam of  $P_R = 38 \text{ mW}$ . The power-beam duration  $t_i$  is varied between 5 to 20 sec. A certain number of spectra recorded after different durations of irradiation are shown in Fig. 8. At the end of one hour, the final crystalline state is obtained. This state is characterized by the narrow peak at 210 cm<sup>-1</sup>. The time evolution of the intensity of this peak is shown in Fig. 9.

Two methods are used to achieve crystallization by a laser beam. The first is continuous irradiation with stepwise changes in the laser power level. The spectra are recorded during irradiation at each power level. These spectra clearly reveal intermediate metastable states. The second method just described above is a time-resolved procedure. The irradiation is applied in short intervals of time  $t_i$  and the recording of the Raman spectra is done after the irradiation time. To induce transformations

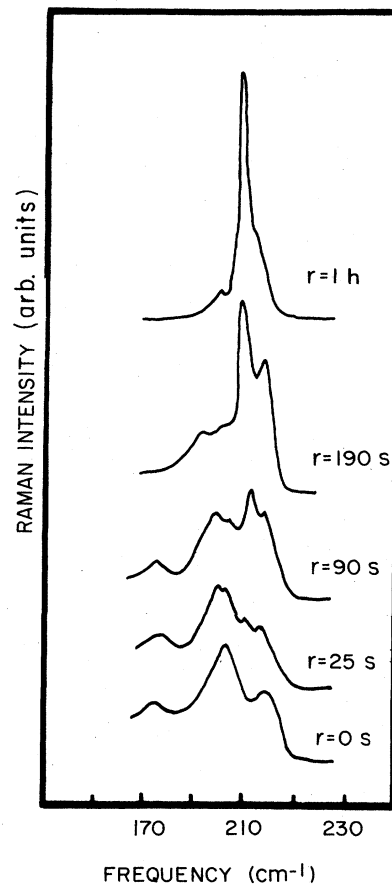


FIG. 8. Detailed dependence of crystallization on exposure time. Irradiation power, 100 mW; recording power, 38 mW.

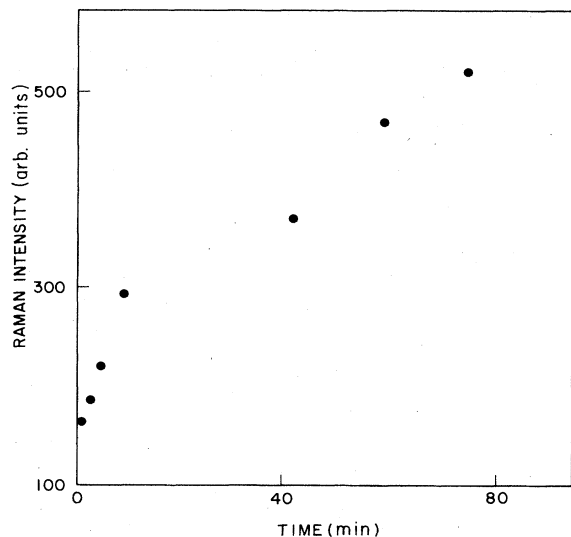


FIG. 9. Strength of the  $210\text{-cm}^{-1}$  crystallization peak in Fig. 8 as a function of time.

analogous to that obtained by continuous irradiation, a certain number of impulses are necessary: the duration of irradiation is a factor in the crystallization of glass.

Transformations in  $g\text{-GeSe}_2$  are also induced<sup>10</sup> by laser irradiation with energy lower than the absorption edge of the material. We have studied the crystallization process in  $g\text{-GeSe}_2$  using an irradiation source of  $E=1.92$  eV. The power in the irradiation beam was increased gradually and the Raman spectra were recorded at different irradiation powers.

The evolution of the Raman spectra as a function of the irradiation power is shown in Fig. 10. Quantitative comparison of spectra 10(a) to 10(d) show a systematic decrease in recorded scattered intensity as the incident irradiation power is gradually increased from 10 to 55 mW. This decrease in the scattered intensity has been interpreted as the photodarkening effect.<sup>10</sup>

In the spectrum 10(d) for which the scattering intensity is minimum, the overall shape of the spectrum changes. The spectrum appears like a broad band evidently because a new peak is growing just between the two peaks of spectrum 10(c) at 200 and 215  $\text{cm}^{-1}$ . When the incident laser power is further increased, this new peak continues to grow in intensity until its scattering intensity becomes so high that it remains the only observable peak as seen in spectrum 10(f). This single peak is now centered at 207  $\text{cm}^{-1}$ .

Photodarkening and laser-induced transformation with a beam at 1.92 eV have been discussed previously<sup>10</sup> and we shall not enter into details here. Although this transformation is similar to that observed with a laser energy of 2.46 eV, one should keep in mind that 1.92 eV is well below the energy gap of  $g\text{-GeSe}_2$  and very few electronic transitions are expected to occur at that energy. On the contrary, 2.46 eV is above the energy gap and band to band transitions are occurring at a rather high rate under irradiation. We have neglected the electronic effect in our

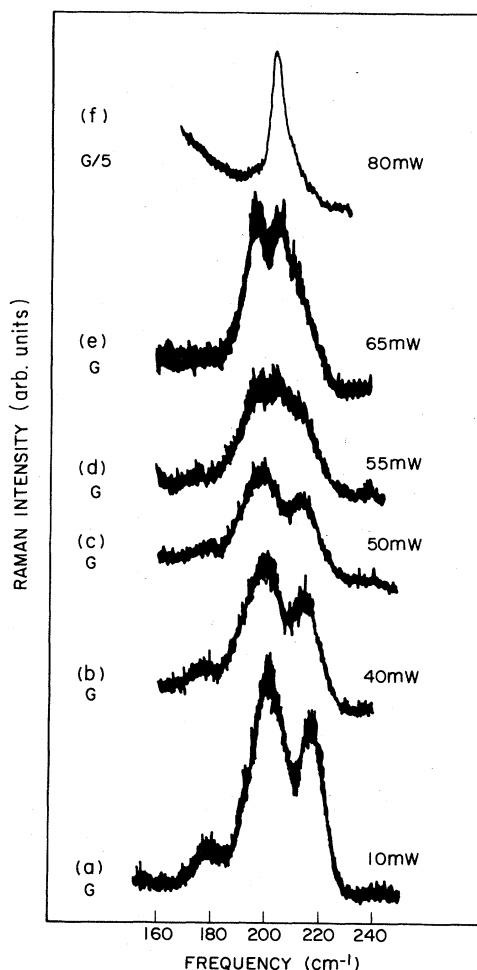


FIG. 10. Crystallization as a function of power level with 1.92-eV beam energy.

discussion until now and the justification for doing so is that we are following here structural changes. There is little we can say about the microscopic origin of these transformations. Undoubtedly bond breaking occurs for energies such as 2.46 eV and the total reorganization of the system might require less power of laser with that energy. The threshold power for the appearance of the new peak is  $E_{th}^{210}=25$  mW at this energy whereas, with lasers at an energy of 1.92 eV, the threshold is at 55 mW ( $E_{th}^{207}=55$  mW). It seems that crystallization occurs more rapidly when induced with a laser of energy higher than the energy gap of the material.

A gradual frequency shift is observed as the irradiation power is increased for the peak at  $210\text{ cm}^{-1}$  as well as for the peak at  $200\text{ cm}^{-1}$ . This variation is shown in Fig. 11 where the frequency at which the Raman line is centered is plotted as a function of the irradiation power. At high irradiation power, the crystalline peak at  $210\text{ cm}^{-1}$  shifts to lower frequencies. It is at  $207\text{ cm}^{-1}$  for a power of  $P_I=110$  mW, and decreases significantly in intensity while broadening at the same time. Figure 12 shows the

line broadening and shift with increasing power of  $P_I = 38$  mW. The Raman peak is centered at  $210\text{ cm}^{-1}$  and has a linewidth  $\Gamma_{210} = 3\text{ cm}^{-1}$ . Spectrum 12(b) is recorded under an incident laser power of  $P_I = 110$  mW. The Raman peak is centered at  $207\text{ cm}^{-1}$ , its intensity is much lower and has a linewidth of  $\Gamma_{207} = 10\text{ cm}^{-1}$ . These effects could be explained by assuming that as the crystallites grow, the free volume increases, and the average internal pressure due to intercrystallite interactions decreases. At the same time inhomogeneities in the internal pressure increase as edges come into contact, which increases the linewidth.

#### F. Reversibility

Irradiation with a laser beam of energy  $E = 2.46\text{ eV}$  and with a power of  $P_I = 38\text{ mW}$  induces the formation of large crystallites whose characteristic vibrational frequency is  $210\text{ cm}^{-1}$ . When the irradiation power is progressively decreased, the intensity of the peak at  $210\text{ cm}^{-1}$  decreases systematically and for low-irradiation power  $P_I = 2.5\text{ mW}$ , this intensity becomes comparable to the intensity of the peak at  $200\text{ cm}^{-1}$ . This inverse transformation is illustrated in Fig. 13. The ratios of intensities are reported in Table I.

If the scattered intensity at  $210\text{ cm}^{-1}$  corresponds to a certain density of crystallites whose size is  $d > 150\text{ \AA}$ , a decrease of this intensity would have the meaning of a decrease in density of such crystallites. What is meaningful here is the ratio of the two peaks:  $210$  and  $200\text{ cm}^{-1}$  attributed, respectively, to large crystallites and microcrystallites. Lowering the irradiation power reverses the trend of organization of the glass. Large crystallites disappear to the benefit of microcrystallites. Increasing the irradiation power leads to the glass to crystalline transformation. When this transformation is stopped at a certain level from which the irradiation laser power is now decreased,

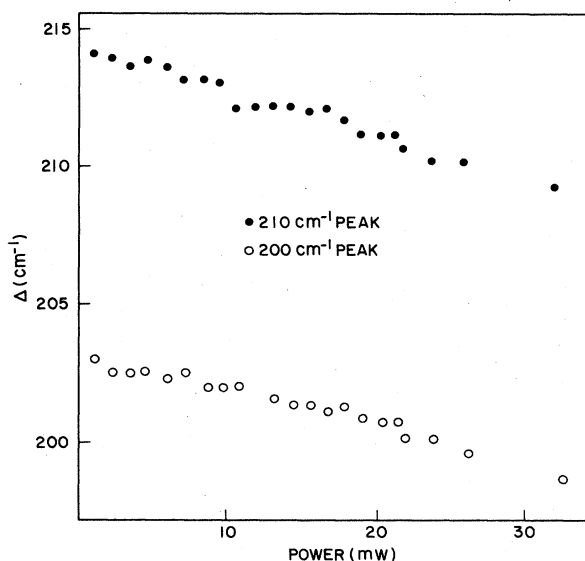


FIG. 11. Relaxation of  $200\text{-cm}^{-1}$  glass and  $210\text{-cm}^{-1}$  crystalline  $A_1$  frequencies with increasing crystallization volume and increasing recording laser beam power.

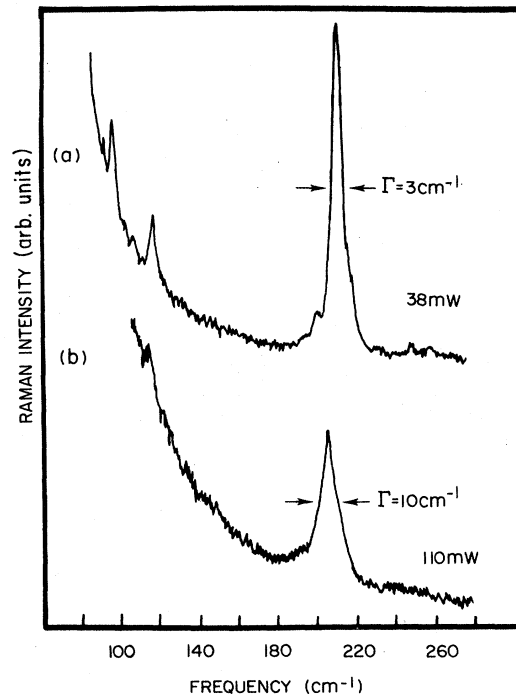


FIG. 12. Narrowing of the crystalline peak with increasing crystallization volume and increasing power levels.

the system seems to reverse: the large crystallites are dissolved in the glass and the microcrystallites tend to dominate.

If one starts from a state at which crystallization has occurred and the peak at  $210\text{ cm}^{-1}$  is the dominant feature of the Raman spectrum, the reversibility is towards a mixed state where crystallites and microcrystallites are both present.

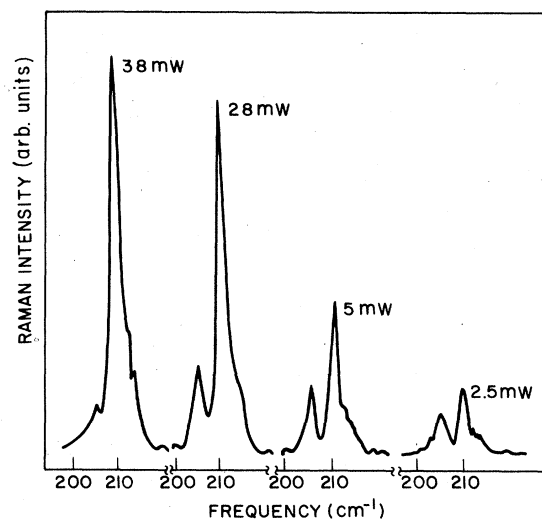


FIG. 13. Reversible partial revitrification with decreasing power level, starting from largely crystallized surface layer and power above threshold.

TABLE I. The ratios of peak intensities for crystallization transformations.

|                           | $P$ (mW)                  |                       |                          |                         |
|---------------------------|---------------------------|-----------------------|--------------------------|-------------------------|
|                           | 38                        | 28                    | 5                        | 2.5                     |
| $\frac{I_{210}}{I_{200}}$ | $\frac{1015}{120} = 8.45$ | $\frac{860}{215} = 4$ | $\frac{383}{170} = 2.21$ | $\frac{158}{94} = 1.68$ |

The situation is quite different when the irradiation is stopped at the level of the precursor effect, i.e., when the  $210\text{-cm}^{-1}$  peak just appears. In this case the reversibility brings the system back to the glassy state. In Fig. 14, spectra recorded with decreasing laser power starting from the level just below the crystallization threshold are shown.

As in the crystallization transformation, there are two stages, one up to the precursor and the second after, crystallization has developed. There are also two levels of reversible transition. Starting from a stage in which a certain degree of crystallization has been induced with a laser beam of decreasing irradiation power, the system is reversible to a stage of balance between microcrystallite and crystallite. If the starting stage is just at the level of the precursor effect, then decreasing irradiation power would bring the system back to the glass state.

## V. CONCLUSION

The experiments discussed here demonstrate some of the possibilities for investigating structural transitions by Raman spectroscopy.

The light scattering spectra recorded after irradiation with an intense laser beam reveal well-defined changes in the structural organization of the glass. A minimum energy density is defined for which the system is not perturbed by the laser irradiation. Beams of this power used to record the light scattering spectra are referred to as probe beams  $P_R$ . The high-energy density beam which induces structural changes in the material is referred to as the pump beam  $P_I$ .

When the energy density of the pump beam is progressively increased, the electromagnetic energy transferred to the system goes either into electronic transitions, i.e., bond breaking or into mechanical transitions, i.e., rotations and vibrations of constituent clusters. This energy transfer into the system results in structural changes in the organization of the material. The experimental results presented here suggest three stages of transformation: the first is nucleation, formation of clusters and increase of their size due to free volume formation up to a stage in which the system consists of clusters—microcrystallites embedded in a continuum glass matrix. This first stage is characterized initially by an increase in intensity of the inner-cluster vibrational band. This is followed by a sharp narrowing accompanied with a further increase of intensity of this same band at  $200\text{ cm}^{-1}$ . The end of this first stage is heralded by a clear precursor effect: the appearance of a new peak at  $210\text{ cm}^{-1}$  as soon as the band at  $200\text{ cm}^{-1}$  has become very narrow:  $\Gamma_{200} = 4\text{ cm}^{-1}$ .

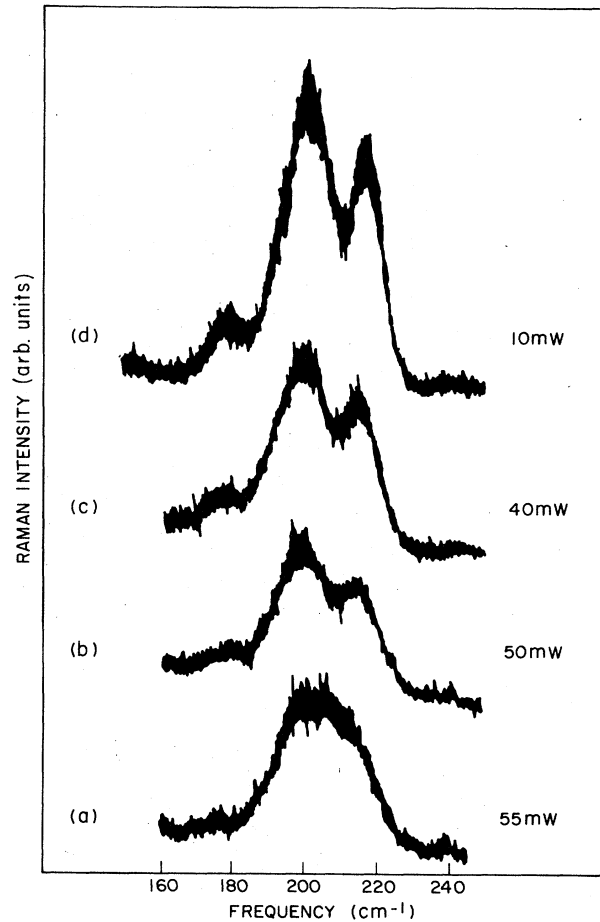


FIG. 14. Complete revitrification starting from precursor power level (below threshold).

The second stage is marked by an intensity effect which expresses the reversible kinetics of the system. During this second stage, the strength of the peak at  $210\text{ cm}^{-1}$ , which is the Raman-active normal mode of  $c\text{-GeSe}_2$ , continuously increases under increasing pump power until it completely dominates the spectrum. At each step of this stage, we observe two peaks,  $200$  and  $210\text{ cm}^{-1}$ , whose relative strength is directly related to the energy density of the pump beam. If at any level of irradiation during this stage the pump beam is removed from the system or its intensity is decreased, the variation in the relative scattering intensity of the two modes  $200$  and  $210\text{ cm}^{-1}$  reverses and reverts toward the more disordered stage and ultimately towards the glass. The second stage is characterized by the persistence of coexisting clusters and microcrystallites, some of which coalesce together to form larger ordered volumes: crystallites of  $d > 150\text{ \AA}$ . At this level, three phases coexist: crystallites, microcrystallites, and glass. The system is that of glass in which clusters of different size cohabit. This stage is attained only by the continuous input of laser energy. When the radiation source is removed, the system relaxes to the glass state with a time delay depending on the amount of energy

which has been previously transferred to the system.

Further increase in the power of the pump beam leads to an increase of the scattering intensity of the mode characteristic for *c*-GeSe<sub>2</sub>. The crystallites coalesce to form crystalline material up to a certain energy input. The system remains relatively reversible. If the pump-beam power is decreased, the scattered intensity of the peak at 210 cm<sup>-1</sup> decreased to the intensity of the peak at 210 cm<sup>-1</sup>. The relaxation of the system in the absence of further irradiation stops at a level which is an equilibrium state between microcrystallite and crystallite.

The third stage is achieved when the system is completely clamped into the crystalline state with a sufficiently long irradiation with a pump beam of high-energy density.

The quantitative relation between intensity of the scattering light and the irradiation power shows two threshold behaviors. The precursor effect is a threshold phenomenon: the scattered intensity of the inner cluster mode at 200 cm<sup>-1</sup> after a very slow variation at low irradiation power suddenly starts to increase extremely rapidly after a threshold energy:  $E_{th}^{200} = 21$  mW. The crystalli-

zation is also a threshold phenomenon. The scattering intensity is practically zero for the peak at 210 cm<sup>-1</sup> below a certain energy density above which this intensity rises extremely rapidly as the irradiation power is increased.

We believe to have given, with this work, a detailed picture of the dynamical evolution of a glass under laser irradiation. This picture is based on three newly demonstrated effects: the precursor effect announcing crystallite formation, the reversible kinematic effect showing equilibrium coexistence between microcrystallite and crystallite under laser irradiation, and the dynamical reversible effect showing two different types of relaxation dependent on the energy input level at which the pumping has stopped.

#### ACKNOWLEDGMENTS

We wish to thank the Consejo Nacional de Ciencia y Tecnología (CONACyT) of Mexico for supporting the work of one of us (E.H.). Laboratoire de Physique des Solides is a Laboratoire associé au Centre National de la Recherche Scientifique, France.

- <sup>1</sup>R. Zallen, M. L. Slade, and A. T. Ward, *Phys. Rev. B* **3**, 4257 (1971).
- <sup>2</sup>R. Zallen and M. L. Slade, *Phys. Rev. B* **9**, 1627 (1974); **9**, 4485 (1974).
- <sup>3</sup>M. L. Slade and R. Zallen, *Solid State Commun.* **30**, 357 (1979).
- <sup>4</sup>B. A. Weinstein, R. Zallen, and M. L. Slade, *J. Non-Cryst. Solids* **35-6**, 1255 (1980).
- <sup>5</sup>B. A. Weinstein, R. Zallen, M. L. Slade, and A. Delozann, *Phys. Rev. B* **24**, 4652 (1981).
- <sup>6</sup>A. Feltz, K. Zichmüller, and G. Pfaff, in *Amorphous and Liquid Semiconductors*, edited by J. Stuke and W. Brenig (Taylor and Francis, London, 1974), p. 125.
- <sup>7</sup>B. A. Weinstein, R. Zallen, M. C. Slade, and J. C. Mikkelsen, *Phys. Rev. B* **25**, 781 (1982).
- <sup>8</sup>K. Murase, T. Fukunaga, K. Yakushiji, and I. Yunoki, *J. Non-Cryst. Solids* **59&60**, 883 (1983).
- <sup>9</sup>P. M. Bridenbaugh, G. P. Espinosa, J. E. Griffiths, J. C. Phillips, and J. P. Remeika, *Phys. Rev. B* **20**, 4140 (1979).
- <sup>10</sup>N. Kumagai, J. Shirafuji and Inuishi, *J. Phys. Soc. Jpn.* **42**, 1261 (1977).
- <sup>11</sup>W. J. Bresser, P. Boolchand, P. Suranyi, and J. P. de Neufville, *Phys. Rev. Lett.* **46**, 1689 (1981).
- <sup>12</sup>P. Boolchand, W. J. Bresser, and M. Tenhover, *Phys. Rev. B* **25**, 2971 (1982).
- <sup>13</sup>P. Boolchand, J. Grothaus, W. J. Bresser, and P. Suranyi, *Phys. Rev. B* **25**, 2975 (1982).
- <sup>14</sup>P. Boolchand, H. Grothaus, and J. C. Phillips, *Solid State Commun.* **45**, 183 (1983).
- <sup>15</sup>M. Stevens, J. Grothaus, P. Boolchand, and J. G. Hernandez, *Solid State Commun.* **47**, 199 (1983).
- <sup>16</sup>A. L. Renninger, M. D. Reichtin, and B. L. Averbach, *J. Non-Cryst. Solids* **16**, 1 (1974); M. D. Reichtin and B. C. Auerbach, *Phys. Status Solidi* **28**, 283 (1975).
- <sup>17</sup>L. Cervinka and A. Hruby, in *Amorphous and Liquid Semiconductors*, Ref. 6, p. 431.
- <sup>18</sup>Further evidence of the unsatisfactory nature of the "rings embedded in a continuous random network" model has been reported for *g*-As<sub>2</sub>S<sub>3</sub> by H. Kawamura, K. Fukumasu, and Y. Hamada, *Solid State Commun.* **43**, 229 (1982).
- <sup>19</sup>J. E. Griffiths, G. P. Espinosa, J. P. Remeika, and J. C. Phillips, *Solid State Commun.* **40**, 1077 (1981); *Phys. Rev. B* **25**, 1272 (1982); J. E. Griffiths, G. P. Espinosa, J. C. Phillips, and J. P. Remeika *ibid.* **28**, 4444 (1983).
- <sup>20</sup>M. Balkanski, E. Haro, G. P. Espinosa, and J. C. Phillips, *Solid State Commun.* **51**, 639 (1984).
- <sup>21</sup>G. I. Kim, N. Kumagai, and J. Shirafuji, *J. Non-Cryst. Solids* **36**, 1047 (1980); D. E. Aspnes, J. C. Phillips, and P. M. Bridenbaugh, *Phys. Rev. B* **23**, 816 (1981).
- <sup>22</sup>J. C. Phillips, *Comments Solid State Phys.* **10**, 165 (1982).
- <sup>23</sup>J. Hajto, G. Zentai, and I. Kosa-Somogyi, *Solid State Commun.* **23**, 401 (1977).
- <sup>24</sup>J. Hajto and P. Apai, *J. Non-Cryst. Solids* **35-6**, 1085 (1980).
- <sup>25</sup>J. Wong and C. A. Angell, *Glass Structure by Spectroscopy* (Dekker, New York, 1976).
- <sup>26</sup>J. C. Phillips, *Phys. Today* **34**, (2), 1, (1982).
- <sup>27</sup>J. A. Aronovitz, J. R. Banaver, M. A. Marcus, and J. C. Phillips, *Phys. Rev.* **28**, 4454 (1983).
- <sup>28</sup>K. Tanaka, S. Kyohya, and A. Odajima, *Thin Solid Films* **111**, 195 (1984), have shown that in As<sub>2</sub>(S,Se)<sub>3</sub> films characteristic dimensions of 500 Å are required to produce photo-darkening. We believe that for smaller dimensions clusters are clamped. See also C. H. Chen, J. C. Phillips, K. L. Tai, and P. M. Bridenbaugh, *Solid State Commun.* **38**, 657 (1981) and *J. Non-Cryst. Solids* **65**, 1 (1984).
- <sup>29</sup>R. Azoulay, *J. Non-Cryst. Solids* **18**, 33 (1975).
- <sup>30</sup>G. Kanellis, J. F. Morhange, and M. Balkanski, *Phys. Rev. B* **21**, 1543 (1980); **28**, 3390 (1983).
- <sup>31</sup>A. R. Yavari, P. Hicter, and P. Desre, *J. Chim. Phys.* **79**, 579 (1982).
- <sup>32</sup>R. W. Cahn, *J. Phys. (Paris) Colloq.* **43**, C9-55 (1982).